Agilent

Trusted Answers

Lipid Profiling Workflow Demonstrates Disrupted Lipogenesis Induced with Drug Treatment in Leukemia Cells

Using an Agilent 6546 LC/Q-TOF and MassHunter Lipid Annotator Software

Authors

Mark Sartain,
Genevieve Van de Bittner, and
Sarah Stow
Agilent Technologies, Inc.
Santa Clara, CA

Abstract

The Agilent lipidomics profiling workflow, using the Agilent 6546 LC/Q-TOF and Agilent MassHunter Lipid Annotator software, was applied to the study of drug-treated acute myeloid leukemia (AML) cells. The results confirmed previously reported observations, and revealed lipid differences made evident through the expanded coverage of this comprehensive workflow.

Introduction

A previous study found that a drug combination (BaP) of the lipid-lowering drug bezafibrate (BEZ) and the contraceptive medroxyprogesterone acetate (MPA) had potent anticancer properties for AML, an aggressive blood cancer.[1] The authors further showed with a series of experiments, including lipid analysis, that BaP slows *de novo* fatty acid and phospholipid biosynthesis through downregulation of lipogenic enzymes, and suggested dysregulation of lipogenesis as a major contributor to the anticancer effect of BaP.

As a proof-of-principle study, we applied a lipidomics profiling workflow to analyze lipid alterations in the AML K562 cell line in response to BEZ, MPA, and the BaP drug combination. The Agilent lipid analysis workflow was performed with the 6546 LC/Q-TOF, a mass spectrometer designed to have wide dynamic range while simultaneously providing improved resolution independent of acquisition rate. Key to the workflow is MassHunter Lipid Annotator software, which quickly annotates lipid MS/MS spectra and easily generates a custom library of detected lipids, with deep annotation coverage. These libraries are a critical component of the complete lipid analysis workflow, and support targeted and untargeted lipidomics profiling.

Experimental

Cell culture

AML K562 cells were cultured in supplemented RPMI medium. Six-well plates were seeded with 2.4×10^5 cells/mL (3 mL/well) and four different treatments were applied: 0.5 mM BEZ, 5 mM MPA, BaP (a combination of 0.5 mM BEZ and 5 mM MPA), or vehicle control (1:1 ethanol/DMSO).

Four replicate wells were prepared for each treatment. After incubation for 24 hours, cells were pelleted by centrifugation, washed with PBS (−Ca, −Mg, 1 mL, 4 °C), repelleted, flash-frozen, and stored at −80 °C. Figure 1 depicts the cell culture strategy.

Lipid extraction

Cell pellets were thawed on ice, and lipids were extracted with a modified Folch extraction procedure. Methanol (200 µL) was added to each cell pellet in a 2 mL Eppendorf tube, and tubes were mixed using a vortex mixer for two minutes. Chloroform (400 µL) was added, and tubes were mixed using a vortex mixer for two minutes. To induce phase partitioning, 120 µL of water was added to each sample. The mixture was then mixed with a vortex mixer for two minutes, and centrifuged at 16,000 × g for five minutes at 4 °C. The lower layer was carefully removed with a gas-tight glass syringe, and transferred to a second Eppendorf tube. To re-extract the remaining interphase and upper phase layers, 450 µL of a chloroform/methanol/water (86:14:1, v/v/v) mixture was added, mixed with a vortex mixer for two minutes, and centrifuged again.
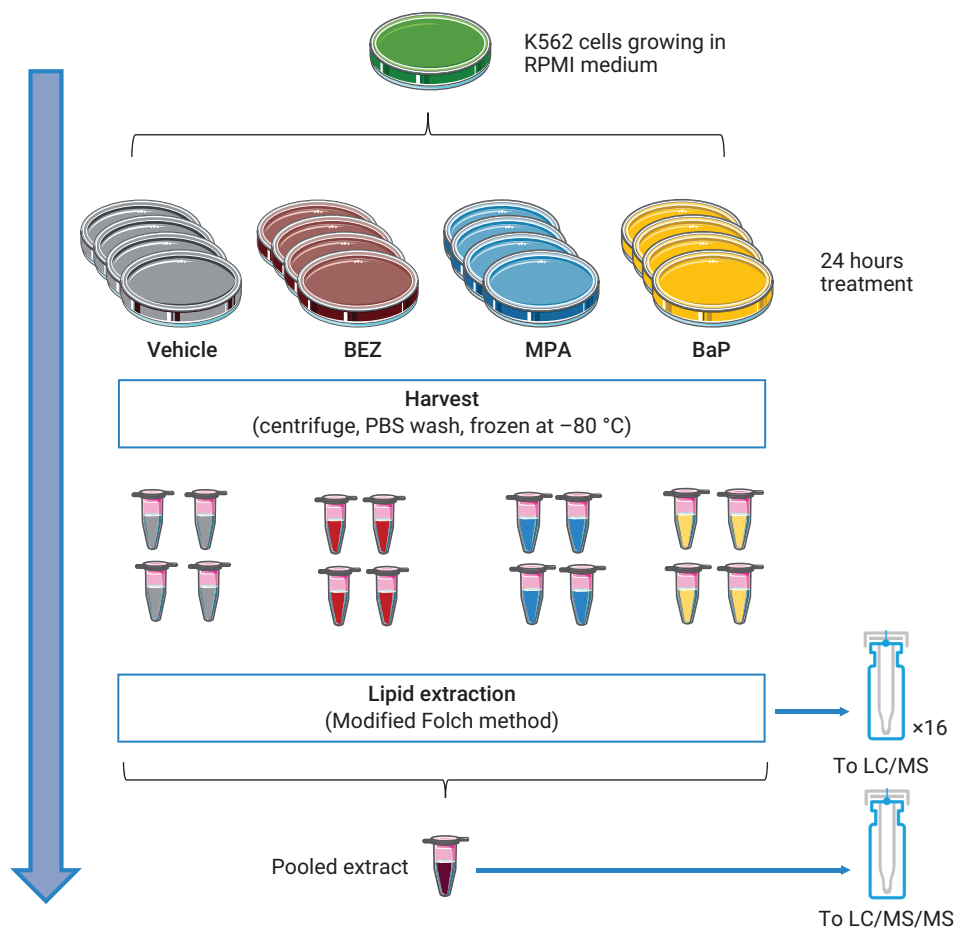

Figure 1. Experimental design for studying effects of drug treatments on cancer cell lipidome.

The lower layers were combined, and 600 µL of a chloroform/methanol/water (3:48:47 v/v/v) mixture was added, the solutions were then mixed using a vortex mixer for two minutes and centrifuged. The lower layer was transferred to a fresh Eppendorf tube, dried by a vacuum concentrator, resuspended with 200 µL of reconstitution solvent (methanol/chloroform (9:1 v/v)), and briefly mixed with a vortex mixer. Extracts were divided and concentrated for different LC/MS acquisition methods as follows:

- Samples for positive ion mode LC/MS:

  1. Fifty microliters of the extracts were transferred to deactivated glass vial inserts for MS1 data acquisition on the individual replicates.

  2. Ten-microliter aliquots from each of the 50 µL samples were combined in a single glass vial insert (16 samples = 160 µL). The pooled aliquot was concentrated by drying in a vacuum concentrator and resuspended in 50 µL of reconstitution solvent for AutoMS/MS (Iterative MS/MS) data acquisition.

- Samples for negative-ion mode LC/MS:

  1. The remaining 150 µL of each extract was transferred to a deactivated glass vial insert and dried by a vacuum concentrator. The samples were resuspended in 50 µL of reconstitution solvent for MS1 data acquisition on the individual replicates.

  2. Ten-microliter aliquots from each of the reconstituted 50 µL samples were combined in a single glass vial insert (16 samples = 160 µL). The pooled aliquot was concentrated by drying in a vacuum concentrator and resuspended in 50 µL of reconstitution solvent for AutoMS/MS (Iterative MS/MS) data acquisition.

- Five-microliter injections were made for all samples.

Instrumentation

- **LC system:** Agilent 1290 Infinity II LC including:

  - Agilent 1290 Infinity II High Speed Pump (G7120A)

  - Agilent 1290 Infinity II Vialsampler with thermostat (G7129B)

  - Agilent 1290 Infinity II Multicolumn Thermostat (G7116B)

- **MS system:** Agilent 6546 LC/Q-TOF with an Agilent Jet Stream technology ion source

Method

A pooled K562 lipid extract representing the 16 samples (four conditions × four replicates) was acquired by Iterative MS/MS, a fully automated Q-TOF acquisition mode in which a sample is injected multiple times, and precursors selected for MS/MS fragmentation in the previous injections are excluded on a rolling basis. The value of Iterative MS/MS in obtaining larger numbers of lipid annotations from a single sample was demonstrated previously.[2]

Detailed experimental methods for chromatography and AutoMS/MS mass spectrometry were followed as described;[2] parameters are provided in Tables 1 and 2. Additionally, MS-only data were acquired on the individual samples, with an MS acquisition rate of three spectra/second.

Table 1. Chromatographic conditions.

Parameter	Agilent 1290 Infinity II LC
Analytical Column	Agilent InfinityLab Poroshell 120 EC-C18, 3.0 × 100 mm, 2.7 µm (p/n 695975-302)
Guard Column	Agilent InfinityLab Poroshell 120 EC-C18, 3.0 × 5 mm, 2.7 µm (p/n 823750-911)
Column Temperature	50 °C
Injection Volume	5 µL
Autosampler Temperature	4 °C
Needle Wash	15 seconds in wash port (50:50 methanol/isopropanol)
Mobile Phase	A) 10 mM ammonium acetate, 0.2 mM ammonium fluoride in 9:1 water/methanol B) 10 mM ammonium acetate, 0.2 mM ammonium fluoride in 2:3:5 acetonitrile/methanol/isopropanol
Flow Rate	0.6 mL/min
Gradient Program	Time %B 0.00 70 1.00 70 3.50 86 10.00 86 11.00 100 17.00 100 17.10 70 19.00 70
Stop Time	19 minutes
Post Time	None
Observed Column Pressure	170 to 330 bar

Software

- Agilent MassHunter Q-TOF Data Acquisition Version 10.0 was used to operate the 6546 LC/Q-TOF.

- Agilent MassHunter Lipid Annotator Version 1.0 with default method parameters was used, except only $[M+H]^+$ and $[M+NH_4]^+$ precursors were considered for positive ion mode analysis, and only $[M-H]^-$ and $[M+HAc-H]^-$ precursors were considered for negative ion mode analysis.

- Agilent MassHunter PCDL Manager Version B.08 SP1 was used to manage and edit the exported annotated lipid libraries (PCDL). Specifically, PCDL Manager was used to remove redundancies for nine Cer_NS lipids, where separate entries were observed for $[M-H]^-$ and $[M+acetate]^-$ molecular ions. The $[M-H]^-$ Cer_NS entries were deleted, leaving 653 lipids in the negative ion mode PCDL.

- Agilent MassHunter Profinder Version 10.0 was used for feature extraction.[3] The provided "Profinder - Lipids.m" method was used for batch targeted feature extraction with the following changes:

  - **Step 1:** +H and +NH4 checked (pos), −H and +CH3COO checked (neg); report single ions or single-ion features with charge state z = 1: checked

  - **Step 2:** Expected data variation for MS isotope abundance: 12.5%

  - **Step 3:** Smoothing function: Quadratic/Cubic Savitzky-Golay with function width 8; height filter: uncheck; limit to largest (by height) to maximum: 10 peaks

Table 2. Agilent 6546 LC/Q-TOF AutoMS/MS (Iterative) parameters.

Parameter	Agilent 6546 LC/Q-TOF
Gas Temperature	200 °C
Gas Flow	10 L/min
Nebulizer (psig)	50
Sheath Gas Temperature	300 °C
Sheath Gas Flow	12 L/min
VCap	3,500 V (+), 3,000 V (−)
Nozzle Voltage	0 V
Fragmentor	150 V
Skimmer	65 V
OctopoleRF Vpp	750 V
Reference Mass	m/z 121.050873, m/z 1221.990637 (+) m/z 119.03632, m/z 980.016375 (−)
MS and MS/MS Range	m/z 40 to 1,700 (+)
Minimum MS and MS/MS Acquisition Rate	3 spectra/s
Isolation Width	Narrow (~1.3 m/z)
Collision Energy	20 eV (+), 25 eV (−)
Maximum Precursors Per Cycle	3
Precursor Abundance-Based Scan Speed	Yes, target 25,000 counts/spectrum
Use MS/MS Accumulation Time Limit	Yes
Reject Precursors that Cannot Reach Target TIC	No
Threshold for MS/MS	5,000 counts and 0.001%
Active Exclusion Enabled	Yes, one repeat, then exclude for 0.05 minutes
Purity	Stringency 70%, cutoff 0%
Isotope Model	Common organic molecules
Sort Precursors	1, 2, unknown
Static Exclusion Ranges	m/z 40 to 151 (+) m/z 40 to 210 (−)
Iterative MS/MS Mass Error Tolerance	20 ppm
Iterative MS/MS RT Exclusion Tolerance	±0.1 minutes

- **Step 4:** Unchanged Step 5 uncheck Score (Tgt)

- Agilent MassHunter Mass Profiler Professional Version 15.1 was used for differential analysis. Two experiments (positive or negative ion) were created with the "Lipidomics" experiment type, and the corresponding Profinder archives (.pfa) were used as the data source. A percentile shift normalization algorithm (75 %) was used, and datasets were baselined to the median of all samples.

- Agilent MassHunter ID Browser Version 10.0 was used within MPP to make annotations in the untargeted workflow, with masses ±5 ppm and retention times ±0.10 minutes as required criteria.

Workflow

Both the targeted and untargeted lipidomics workflows were used as previously described.[4]

Results and discussion

Lipid Annotator database creation with pooled AML cellular lipid extracts

As the first step in the lipidomics workflow, two sets of five Iterative MS/MS data files from pooled AML cell extracts were analyzed with Lipid Annotator software (Figure 2). There were 430 lipids representing 17 classes annotated for positive ion mode, and 653 lipids representing 25 classes annotated for negative ion mode. Lipid Annotator results were exported to PCDL (.cdb) files.
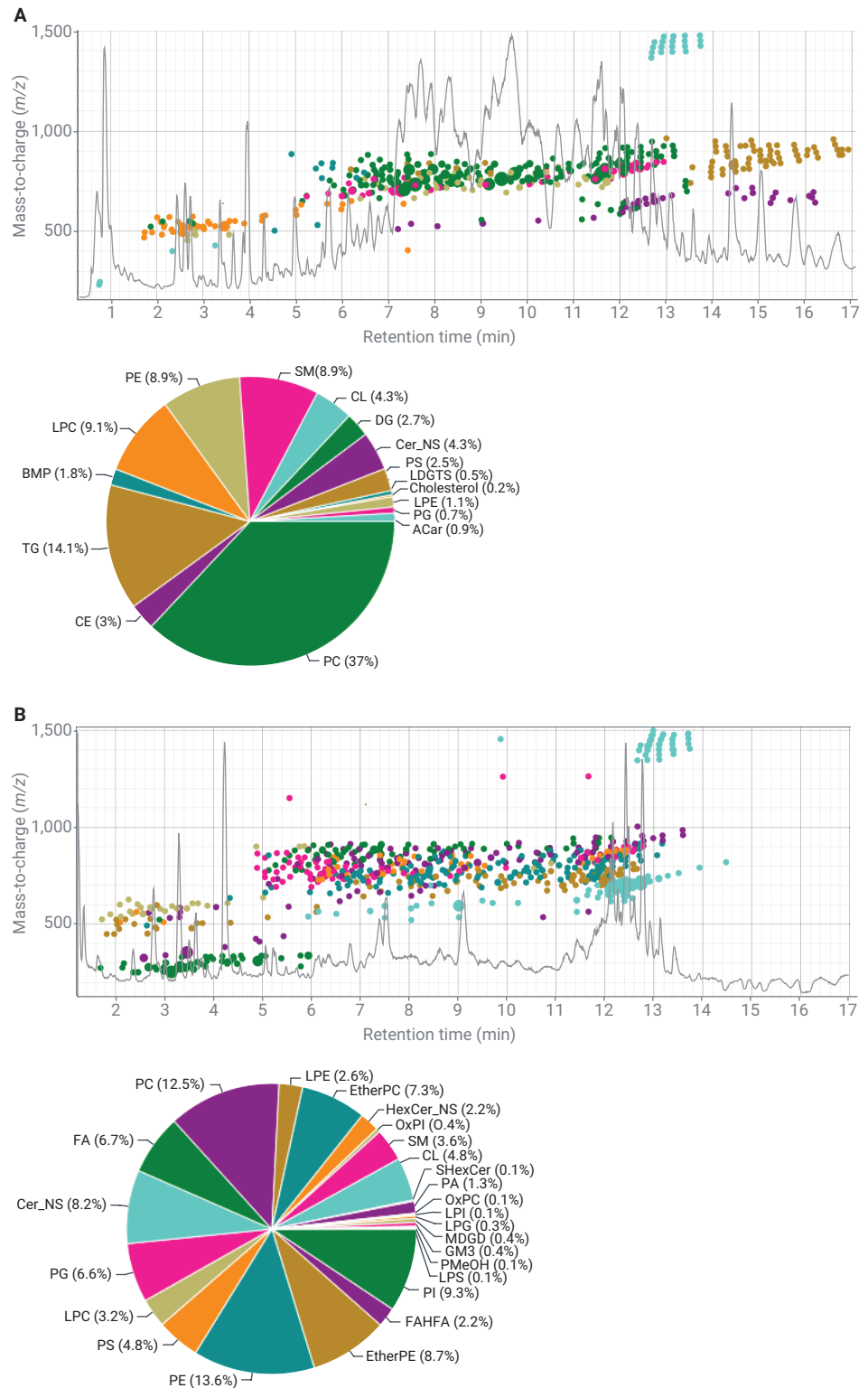
Figure 2. Lipid Annotator software results for positive (A) and negative (B) ionization modes. Five Iterative MS/MS data files were analyzed as a batch for each project. For illustration purposes, a representative total ion chromatogram is overlaid with the *m/z* versus retention time scatter plot. Lipid features are colored by lipid class corresponding to the pie charts, where the numbers of annotated lipids are shown as percentages.

Lipid profiling identifies perturbations induced with drug treatments

The PCDL (.cdb) databases were used for Batch Targeted Feature Extraction in Profinder on the respective batches of 16 MS1 data files. Critically, both the database compound formulas and retention times were used as required criteria to search the MS1 data files for the lipid features in a targeted manner. Resulting compounds were reviewed in Profinder and, in some cases, features were manually integrated or removed due to poor or ambiguous feature peak shapes. After manual curation, 375 compounds and 548 compounds remained in the positive and negative ion mode datasets, respectively. Profinder results (.pfa file) were imported into Mass Profiler Professional (MPP) for statistical analysis, where separate experiments were created for positive and negative ion modes. After normalization and baselining, the resulting PCA plots for both polarities were similar. Without filtering of entities (keeping all compounds), the results showed tight clustering of the biological replicates within each condition and demonstrated clear differences between the drug treatments. Both BEZ and MPA contributed separately to the combination BaP effect (Figure 3). Separation of the groups along principal component 1 suggested that BEZ treatment contributed more than MPA to the combination BaP drug effect on the lipidome. These observations were consistent with those described previously.[1]
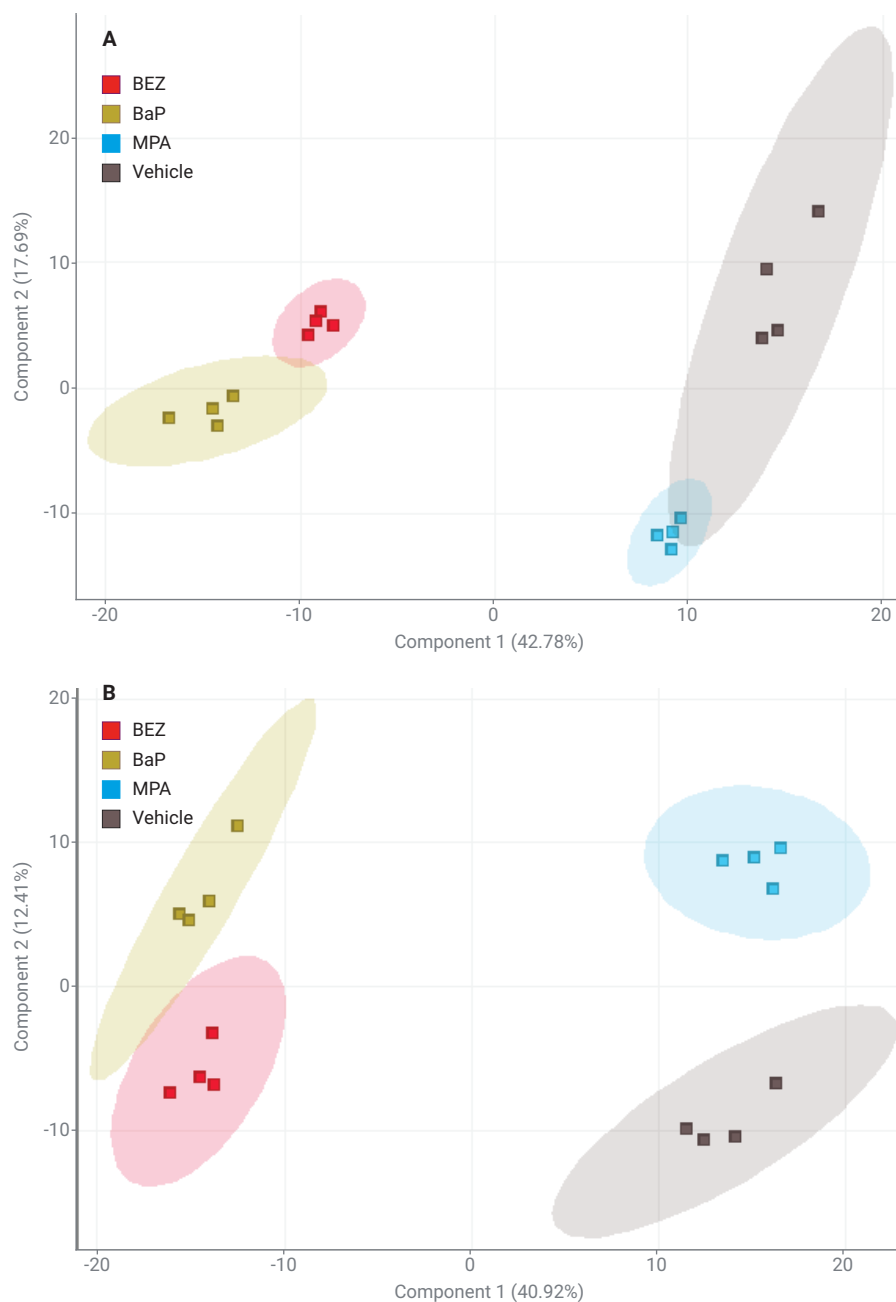

Figure 3. PCA plots for the positive ion (A) and negative ion (B) datasets.

Sample correlation (not shown) and unsupervised hierarchical clustering (Figure 4) provided further support for the PCA results. Biological replicates within the conditions grouped together, and BEZ samples showed a closer relationship to BaP than MPA samples. Trends were also observed from unsupervised clustering on the annotated lipid features. For example, inspection of the cluster tree within a region showing a clear pattern revealed a close relationship for many triacylglycerol (TG) lipids. These lipids were increased in BEZ and BaP treatments compared to MPA and the vehicle control samples.
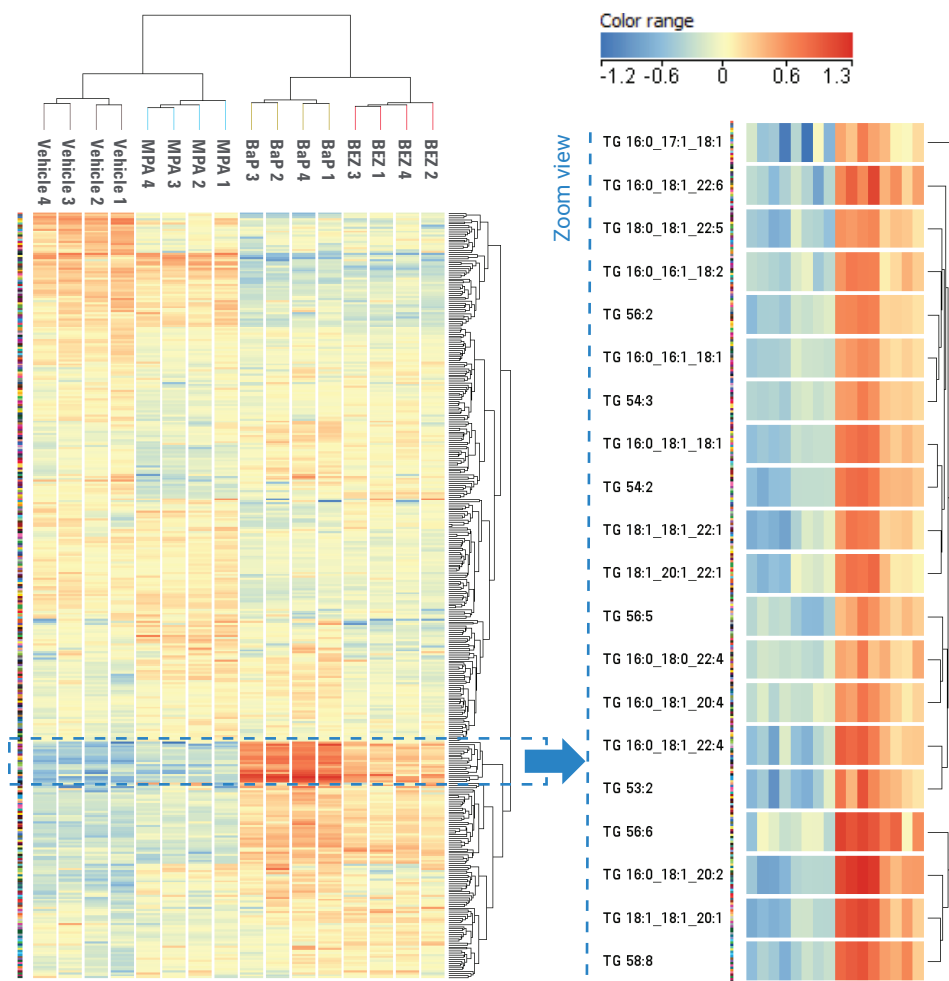

Figure 4. Combined unsupervised hierarchical clustering results on compounds (n = 375) and conditions for the positive ion dataset. (Right) A zoomed region of the cluster tree enriched with annotated TG lipids is shown. The color range represents the normalized, transformed abundances for each TG feature represented on a log2 scale.

Lipid profiling demonstrates disrupted lipogenesis

To assess differences across lipid class abundances in more detail, a lipid class matrix plot (heat map) was created in MPP from the positive ion mode dataset (Figure 5). Clear differences were observed. In agreement with Southam *et al.*,[1] TGs were increased and diacylglycerols (DGs) were decreased in BaP versus vehicle control. DGs are intermediates in the *de novo* phospholipid biosynthetic pathway, and the authors suggested that DG depletion with BaP treatment resulted from disruption of phospholipid synthesis at the acyl chain addition stage. Table 3 shows a summary of lipid classes with significantly different abundances from the positive and negative ion datasets.

In contrast to the previous report, we did not observe a significant decrease of lysophosphatidylcholine (LPC) or lysophosphatidylethanolamine (LPE) class abundances with BaP treatment. Multiple reasons could account for this discrepancy, including differences in normalization and processing methods for the MS lipid datasets. We observed significant lipid class differences not reported in the previous study, most notably increases in levels of ceramide nonhydroxyfatty acid-sphingosines (Cer_NS) and hexosylceramide nonhydroxyfatty acid-sphingosines (HexCer_NS), and decreased phosphatidylcholine (PC) levels in BaP treated cells versus vehicle control. While the previous study applied a shotgun lipidomics approach with targeted scans for a limited panel of lipid classes, our targeted workflow began with a discovery phase to search a comprehensive *in silico* spectral library, and then used these results for targeted data mining. Therefore, our approach was unrestricted, and likely led to these findings in lipid class differences.
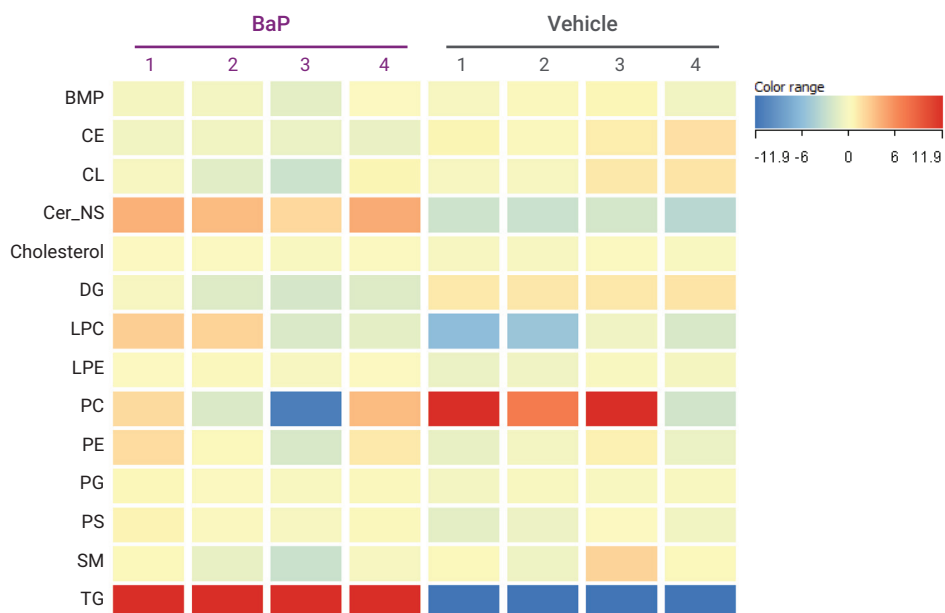

Figure 5. MPP lipid class matrix of total normalized lipid class abundances across BaP treatment and vehicle control sample replicates. The color range represents the sum of normalized, transformed abundances for all lipid features within a lipid class.

Table 3. Summary of lipid classes with significantly different abundance levels induced with BaP treatment.

Lipid Class	Abbreviation	BaP Effect	Polarity†
Ceramide Nonhydroxyfatty Acid-Sphingosines	Cer_NS	Increased	(+)***, (-)*
Hexosylceramide Nonhydroxyfatty Acid-Sphingosines	HexCer_NS	Increased	(-)***
Triacylglycerols	TG	Increased	(+)***
Gangliosides	GM3	Increased	(-)**
Lyso-Phosphatidylglycerols	LPG	Increased	(-)**
Ether-Linked Phosphatidycholines	Ether PC	Increased	(-)*
Lyso-Phosphatidylethanolamines	LPE	Increased	(+)*
Lyso-Phosphatidylserines	LPS	Increased	(-)*
Sulfatides	SHexCer	Increased	(-)*
Diacylglycerols	DG	Decreased	(+)***
Monogalactosyldiacylglycerols	MGDG	Decreased	(-)***
Phosphatidylinositols	PI	Decreased	(-)***
Cholesterol Esters	CE	Decreased	(+)**
Cardiolipins	CL	Decreased	(-)**
Oxidized Phosphatidylcholines	OxPC	Decreased	(-)*
Oxidized Phosphatidylinositols	OxPI	Decreased	(-)*
Phosphatidic Acids	PA	Decreased	(-)*

† A two-tailed t-test was used to determine significance between vehicle and BaP sample groups:
* $p < 0.05$, ** $p < 0.01$, *** $p < 0.001$

Lipid matrices were also created in MPP to visualize abundance differences across individual lipid features within lipid classes. Inspection of the phosphatidylcholine (PC) matrix plot revealed some inverse patterns corresponding to a decrease in PCs with saturated fatty acyl chains (for example, PC 16:0_26:0) and an increase in PCs with polyunsaturated fatty acyl chains (for example, PC 18:1_22:6) induced with BaP treatment (Figure 6). These observations are also consistent with Southam et al.,[1] who suggested that PC lipids with 0 to 2 double bonds are decreased due to reduced de novo fatty acid and phospholipid synthesis induced by BaP treatment. They further hypothesized that the increase in polyunsaturated PC lipids was most likely due to cells obtaining polyunsaturated fatty acids from an exogenous source other than glucose.

Differential response of lipid isomers with drug treatment

The comprehensive LC-based lipidomics approach allowed profiling of lipid isomers that had the same sum composition (that is, same exact mass) but were resolved with chromatography. There were significant numbers of such isomers in the datasets: in the positive mode dataset, 94 of the 430 annotated lipids were isomers, while in the negative mode dataset, 165 of 653 annotated lipids were isomers. In many cases, isomers showed markedly different responses to drug treatment. Inspection of the ceramide (Cer_NS) lipid matrix in MPP revealed an inverse relationship for several pairs of isomers (Figure 7A). As an example, extracted ion chromatograms for the pair of partially resolved Cer_NS 42:2 isomers confirmed an inverse response to BaP treatment, where the later-eluting isomer was decreased in BaP treatment compared to the early-eluting isomer (Figure 7B).
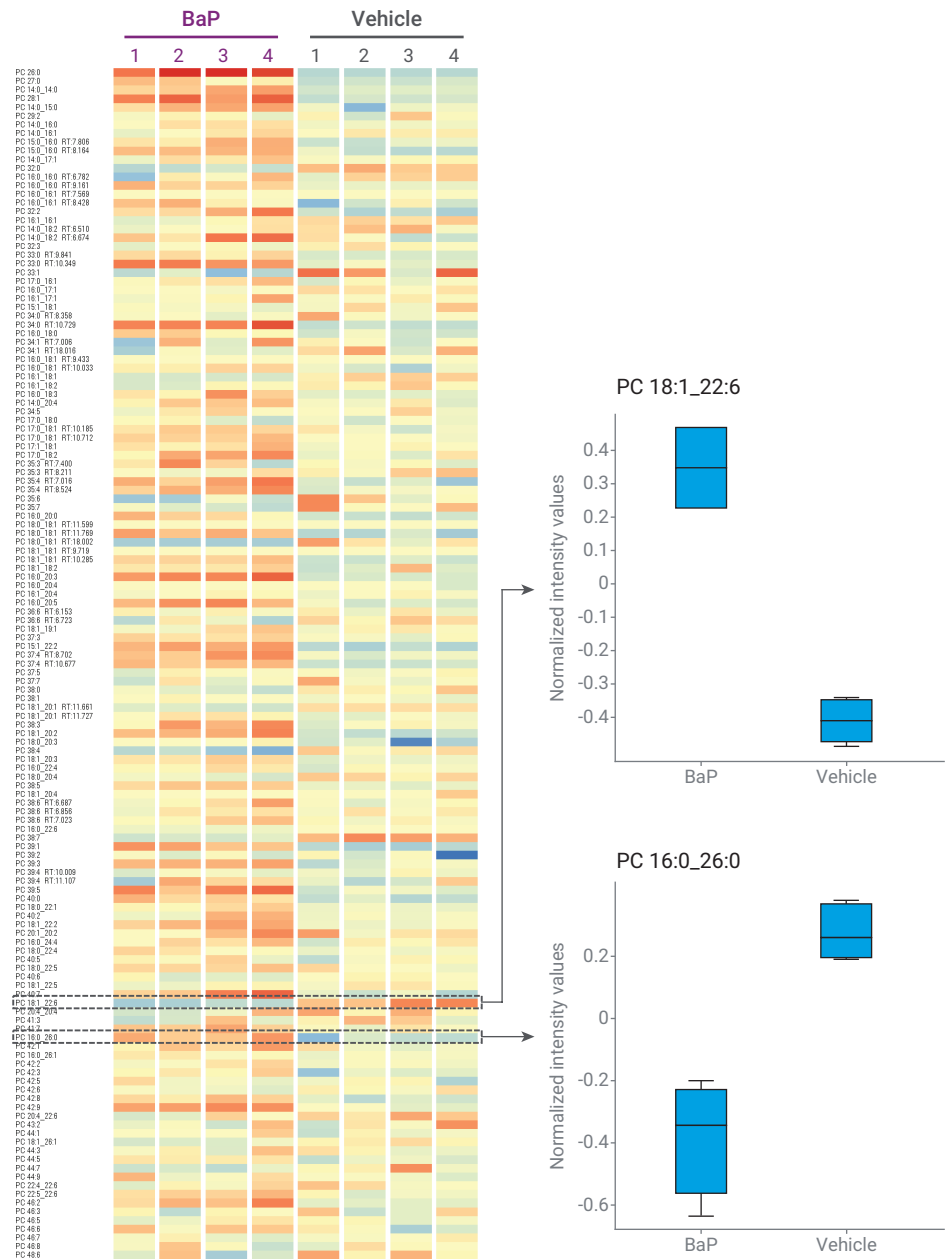
Figure 6. MPP lipid matrix of 137 phosphatidylcholine (PC) lipid features across BaP treatment and vehicle control sample replicates. Box and whisker plots of two selected PC features are shown to the right.
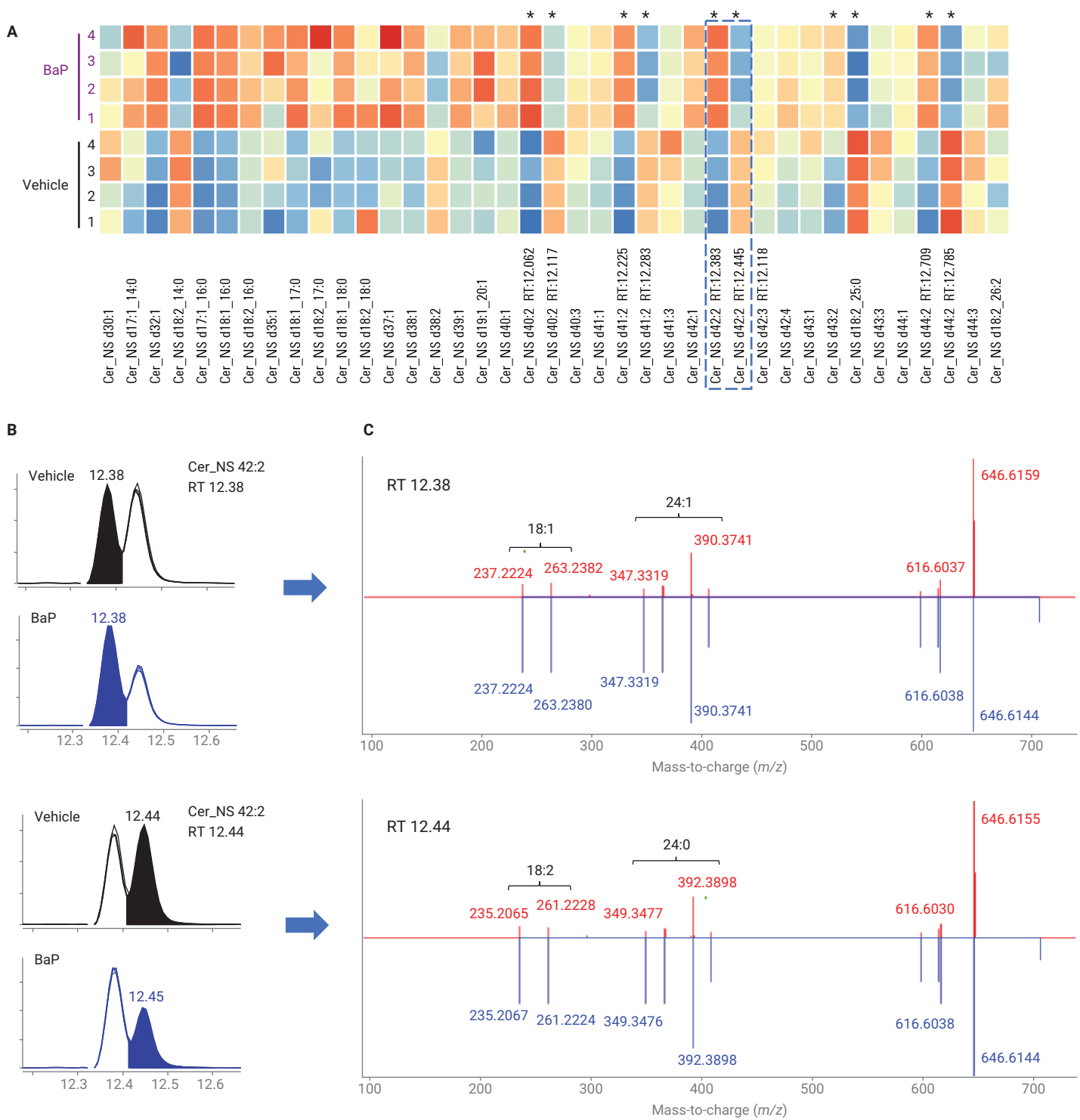
Figure 7. Differential responses and structural elucidation of ceramide nonhydroxyfatty acid-sphingosine (Cer_NS) isomers. (A) MPP lipid matrix of 39 Cer_NS lipid features across BaP treatment and vehicle control sample replicates. Pairs of isomers indicated with asterisks have the same exact mass but different retention times and showed an inverse response. (B) Overlaid extracted ion chromatograms comparing vehicle control (n = 4) to BaP treatment (n = 4) for the pair of Cer_NS 42:2 isomers. (C) Corresponding head-to-tail plots from Lipid Annotator with the major matched product ions additionally labeled (observed, red; database values, blue). Product ion shifts of plus or minus *m/z* 2.0156 between the two plots provided the evidence for the difference in the double bond numbers in the sphingosine bases and esterified fatty acids (labeled). The observed spectra matched Cer_NS d18:1_24:1 and Cer_NS d18:2_24:0 database spectra, and these were indicated as the most likely constituents in the Lipid Annotator software.

While the isomers were annotated with the same sum composition, inspection of Lipid Annotator results provided strong evidence that the early- and late-eluting isomers were Cer_NS d18:1_24:1 and Cer_NS d18:2_24:0, respectively (Figure 7C). The biological significance of the differential response of ceramide isomers to BaP treatment is not known, but this type of information is only revealed with the lipidomics profiling approach.

The untargeted lipidomics workflow reveals a highly differential atypical lipid

As described elsewhere,[4] untargeted workflows are also supported and use the same PCDL and software as the targeted workflow previously described. The major differences are that:

- Untargeted feature finding (recursive batch feature extraction algorithm) in Profinder is used, and

- Lipid annotation is performed later in the workflow within MPP using the ID Browser tool.

In our study, the 16 negative ion MS1 data files were analyzed with the recursive batch feature extraction algorithm in Profinder, and 2,052 features were imported into MPP. As a result, 513 out of the 2,052 features were annotated as lipids with the ID Browser tool using the same negative-ion PCDL library created above (RT ±0.10 minutes was specified as the required criteria).

To focus the differential analysis on reproducible features, the entity list was filtered by sample variability with a CV <25% required for all four conditions. This reduced the entity list to 1,377 features. A moderated t-test on BaP treatment versus vehicle control resulted in 93 entities that were significantly different (fold-change cutoff 1.5, p-value 0.05), and 41 of these entities had been annotated as lipids (Figure 8A). The most highly differential feature showed a 3.93-fold increase in BaP cells compared to vehicle control (p-value 3.54×10^{-5}), and inspection of the entity showed striking differences across the four conditions (Figure 8B). The compound of interest had a neutral mass of 339.2774 Da, and ID Browser did not return an annotation.

To gain insight into the nature of this compound, a Kendrick mass defect (KMD) plot was created in MPP for the combined list of 513 annotated lipids and the 93 differential entities (Figure 8C). Plotting KMD (Y-axis) against lipid class (X-axis) revealed that the feature of interest shared a similar KMD to a group of four Cer_NS lipids each with two double bonds. Interestingly, the masses of the four ceramide lipids (masses 707 to 735 Da) were much larger than the feature of interest (339 Da). The Lipid Calculator tool within Lipid Annotator was used to generate hypothetical Cer_NS lipids to assess whether a sum composition could be generated with a resulting mass close

to m/z 339.2774. With this approach, the lipid Cer_NS d18:2_2:0 showed a mass within 0.3 ppm of the observed feature mass. Furthermore, analysis with Qualitative analysis software showed an MS/MS product ion specific for the d18:2 sphingosine backbone that provided further evidence for the candidate Cer_NS d18:2_2:0 annotation (data not shown). The candidate structure for Cer_NS d18:2_2:0, also known as C2 ceramide or N-acetylsphingosine, is shown in Figure 8D. This C2 ceramide is absent in many lipid databases (including Lipid Annotator) and, to our understanding, has not routinely been identified in lipidomics studies. However, C2 ceramide was found physiologically at low levels in a different AML cell line (HL-60).[5] Synthetic C2 ceramide is widely used as a research tool for its biologically active properties, including the ability to inhibit cell proliferation and induce apoptosis.[6] We speculate the increase of C2 ceramide in the BaP-treated cells could be related to the anticancer effects of BaP, and believe this information may be of interest to the cancer research community.
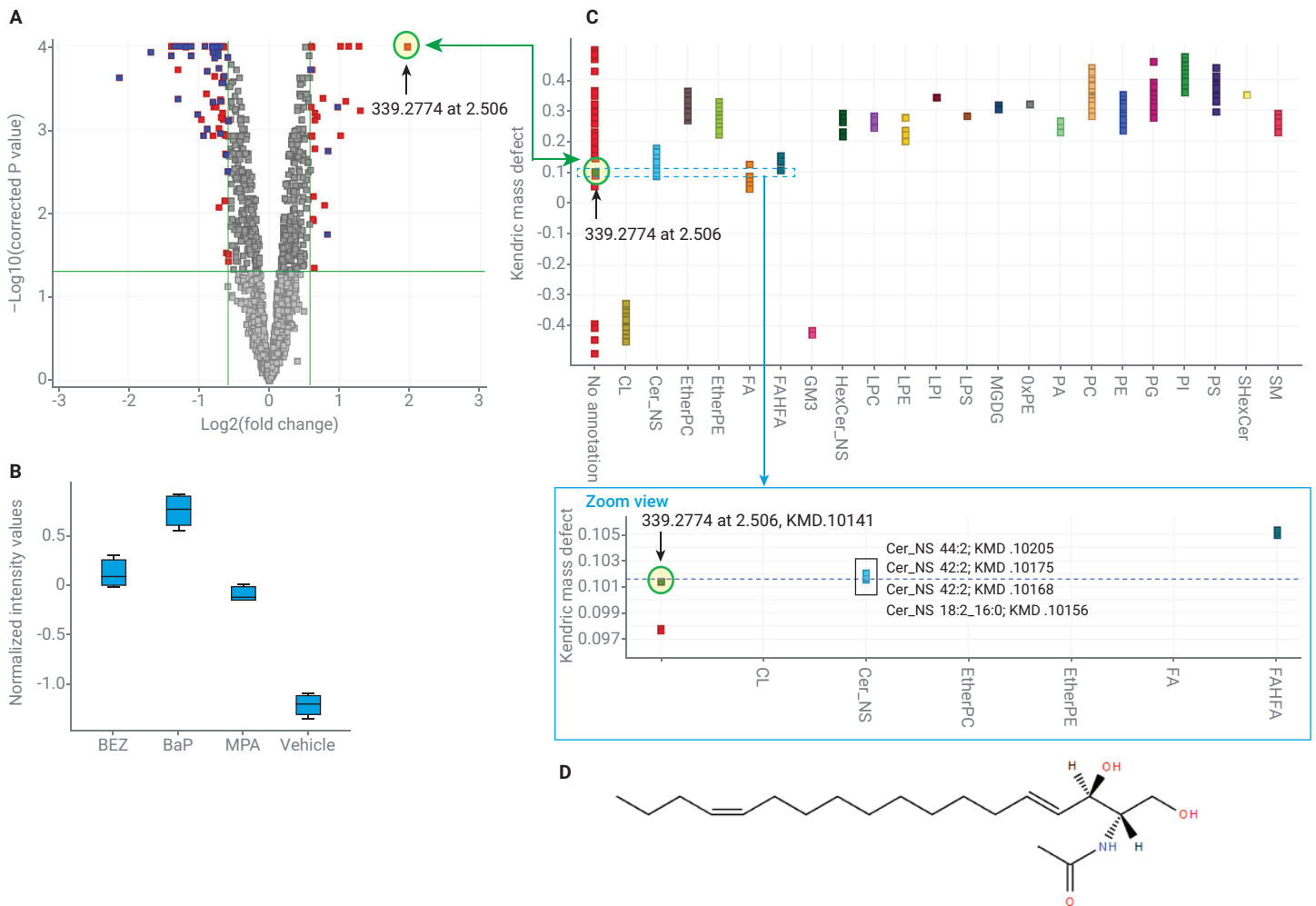
Figure 8. Elucidation of an unknown differential feature with the untargeted workflow. (A) MPP Volcano plot from a moderated t-test with Benjamini-Hochberg FDR multiple testing correction for BaP treatment versus vehicle control. Significant features (fold change cutoff >1.5, p-value >0.05) are colored in blue (annotated lipids) and red (unannotated features). The feature of interest (*m/z* 339.2774 at 2.506) is circled in green. (B) Box and whisker plot of the feature of interest for the four drug treatment conditions. (C) MPP Kendrick mass defect (KMD) plot for the combined entity list of 513 annotated lipids with the list of 93 differential features (n = 565). Features that could not be annotated with the PCDL are shown in the first column in red. The zoomed region shows the alignment by KMD of the feature of interest with a group of Cer_NS lipids. (D) Cer_NS 18:2_2:0 candidate structure for the feature of interest.

Conclusion

This Application Note demonstrates that the lipidomics profiling workflow, including Lipid Annotator software, provides substantial improvement in lipid annotation and differential analysis of complex samples. We applied a targeted workflow to study lipidome alterations of the acute myeloid leukemia K562 cell line in response to a combination of the BEZ and MPA drug candidates. The resulting analysis revealed several cellular changes in response to drug treatment, including a decrease in diacylglycerols, an increase in triacylglycerols, and differences in fatty acyl components. Taken together, these results support a previous report suggesting that the BaP combination may exert its anticancer properties through disruption of lipogenesis.

This lipid profiling workflow also provides more comprehensive lipid annotation than can be achieved by traditional shotgun-based lipidomics approaches. Specifically, we identified significant differences in lipid class abundances induced with BaP treatment that were not previously reported. We also identified specific cases of chromatographically separated lipid isomers that displayed differential responses to drug treatment. Finally, with an untargeted approach we demonstrated the ability to propose candidate annotations for unannotated lipid features using supplementary tools.

References

1. Southam, A. D. *et al.* Drug Redeployment to Kill Leukemia and Lymphoma Cells by Disrupting SCD1-Mediated Synthesis of Monounsaturated Fatty Acids. *Cancer Res.* **2015**, *75(12)*, 2530–2540.

2. Sartain, M. *et al.* Improving Coverage of the Plasma Lipidome Using Iterative MS/MS Data Acquisition Combined with Lipid Annotator and 6546 LC/Q-TOF. *Agilent Technologies Application Note*, publication number 5991-0775EN, **2019**.

3. MassHunter Profinder: Batch Processing for High-Quality Feature Extraction of Mass Spectrometry Data. *Agilent Technologies Technical Overview*, publication number 5991-3947EN, **2014**.

4. Lipidomics Analysis with Lipid Annotator and Mass Profiler Professional. *Agilent Technologies Technical Overview*, publication number 5994-1111EN, **2019**.

5. Snyder, F. *et al.* Biosynthesis of N-Acetylsphingosine by Platelet-activating Factor: Sphingosine CoA-independent Transacetylase in HL-60 Cells. *The Journal of Biological Chemistry* **1996**, *271(1)*, 209–217.

6. Hannun, Y. A. *et al.* Programmed Cell Death Induced by Ceramide. *Science* **1993**, *259(5102)*, 1769–1771.

www.agilent.com/chem

Agilent
Trusted Answers